RECONSTRUCTION OF SCALAR DIFFRACTION FIELD FROM DISTRIBUTED DATA POINTS OVER 3D SPACE

G. Bora Esmer[1], Vladislav Uzunov[2], Levent Onural[1], Atanas Gotchev[2] and Haldun M. Ozaktas[1]

[1] Bilkent University, Department of Electrical and Electronics Engineering,
TR-06800 Ankara, Turkey
[2] Tampere University of Technology, Institute of Signal Processing, FIN-33101 Tampere, Finland

ABSTRACT

Diffraction field computation is an important task in the signal conversion stage of the holographic 3DTV. We consider an abstract setting, where the diffraction field of the desired 3D scene to be displayed is given by discrete samples distributed over 3D space. Based on these samples, a model of the diffraction field should be built to allow the field computation at any desired point. In our previous works, we have proved our concepts for the simplistic 2D case. In this paper, we generalize the earlier proposed techniques, namely the projection onto convex sets and conjugate gradient based techniques and test them for their computational efficiency and memory requirements for a specific 3D case.

Index Terms— Scalar Optical Diffraction, Rayleigh - Sommerfeld Diffraction, Plane Wave Decomposition, Projection onto Convex Sets, Conjugate Gradient

1. INTRODUCTION

Holographic 3DTV requires the following basic building blocks: capture, representation, coding, signal conversion and display. In this chain, the display device plays a very important role, as it generates the light field being the optical replica of the captured and abstractly represented 3D scene. This work is related with the signal conversion part which provides the connection between the 3D scene representation and the display end.

In diffraction theory, computation of a diffraction field at a surface due to a given field elsewhere is one of the major problem which has attracted researchers for decades [1]. Computation of the scalar optical diffraction due to an abstract 3D scene is a challenging problem.

In this work, we assume that a 3D scene is described by a set of distributed data points over the 3D space. In our earlier works [2], [3], this problem has been addressed within a 2D space and now it is extended to 3D space. Problems computational complexity and memory management arising with this extended space setting, are commented in more details.

2. BASICS OF THE SCALAR OPTICAL DIFFRACTION THEORY

To compute scalar optical fields, we do not use Fresnel or Fraunhofer approximations. Instead, we rely on the Rayleigh-Sommerfeld (R-S) integral as the more general and exact scalar optical diffraction integral. More specifically, we utilize the plane wave decomposition (PWD) since it provides the same result as the R-S diffraction integral [4]. While the latter utilizes spatial domain relations, the former interprets the problem in frequency domain and is more attractive from computational point of view. The notations in this work are generalized from [2] and [3].

Lets assume that an initial diffraction field, $u_a(x, y, 0)$, is given on the plane $z = 0$. 2D Fourier transform (FT) of $u_a(x, y, 0)$ gives the complex coefficients of the plane waves, $A(k_x, k_y)$, that form $u_a(x, y, 0)$,

$$(2\pi)^2 A(k_x, k_y) = \mathcal{F}\{u_a(x, y, 0)\} \tag{1}$$

where $\mathcal{F}$ denotes the 2D FT [5]. Then, the diffraction field for monochromatic waves on another plane which is parallel to $z = 0$ is expressed as

$$u_a(x, y, z) = \int\limits_{-\frac{2\pi}{\lambda}}^{\frac{2\pi}{\lambda}} A(k_x, k_y) \exp\left[j(k_x x + k_y y + k_z z)\right] dk_x dk_y \tag{2}$$

where k_x, k_y and k_z are the spatial frequencies of the propagating waves along the directions x, y and z axes, respectively. The **x** and **y** axes denote the transversal directions and **z** is the longitudinal axis which is the optical axis. The variable k_z can be expressed as a function of k_x and k_y, because of dealing with monochromatic waves, $k_z = \sqrt{k^2 - k_x^2 - k_y^2}$, where $k = \frac{2\pi}{\lambda}$.

The spatial frequencies of the diffraction field which is propagating along the optical axis may be restricted to be within $-B \leq k_x, k_y \leq B$, where $B \leq k$. For numerical computations the frequencies k_x and k_y are discretized to N frequency terms each. Consequently, the input signal can be represented by N^2 frequency components. These frequency components are selected as $k_x = n_f \frac{2B}{N}$ and $k_y = m_f \frac{2B}{N}$,

where n_f and m_f are integers and elements of the set $[-N/2, N/2]$. Uniform sampling operation in frequency domain causes periodicity in the transversal spatial domain. The period in both **x** and **y** axes is $X = \frac{\pi N}{B}$. Therefore, the expression given by Eq. 2 becomes

$$u_a(x, y, z) = \sum_{n_f=-N/2}^{N/2-1} \sum_{m_f=-N/2}^{N/2-1} A_D(n_f, m_f)$$
$$\exp\left(j\sqrt{k^2 - (\frac{2B}{N}n_f)^2 - (\frac{2B}{N}m_f)^2}z\right)$$
$$\exp\left[j\frac{2B}{N}(n_f x + m_f y)\right] \tag{3}$$

where $A_D(n_f, m_f)$ is a 2D array representing samples of $A(k_x, k_y)$ [6]. Sampling along the **x** and **y** axes is accomplished by setting the sampling period $X_s = \frac{\pi}{B}$ to satisfy the Nyquist rate. Therefore, the expression in Eq. 3 can be rewritten as

$$u_a(nX_s, mX_s, pX_s) = \sum_{n_f=-N/2}^{N/2-1} \sum_{m_f=-N/2}^{N/2-1} A(n_f, m_f)$$
$$H_p(n_f, m_f) \exp\left[j\frac{2\pi}{N}(n_f n + m_f m)\right] \tag{4}$$

where $H_p(n_f, m_f)$ is the frequency response of the free space propagation kernel, which is defined as

$$H_p(n_f, m_f) = \exp\left(j\frac{2\pi}{N}\sqrt{\beta^2 - n_f^2 - m_f^2}p\right), \tag{5}$$

where $\beta = \frac{NX_s}{\lambda}$ and $p = \frac{z}{X_s}$. Thus the discrete diffraction field becomes,

$$u(n, m, p) = DFT^{-1}\{DFT\{u(n, m, 0)\}H_p(n_f, m_f)\}, \tag{6}$$

where DFT and DFT^{-1} stand for discrete FT and inverse discrete FT, respectively [6].

3. DISCRETE FIELD COMPUTATION FROM DISTRIBUTED DATA

Two methods are presented: projection onto convex sets (POCS) and conjugate gradient (CG). Both of them take the given distributed sample points as an input and give the diffraction field on a reference plane. We choose to implement these fast iterative methods, because direct solution needs much more computation time.

3.1. Projection Onto Convex Sets

First method is based on an iterative approach POCS. Our problem falls in the framework of POCS as proven in [2]. The constraints for the problem are the given samples and the R-S diffraction field relationship. The algorithm utilizes Eq. 6.

The summary of the algorithm is

1. initialize the first line of the desired field $f(n_{i_1}, m_{i_1}, 1) = \mathbf{v}_1$, $f(n_{\bar{i}_1}, m_{\bar{i}_1}, 1) = q(n_{\bar{i}_1}, m_{\bar{i}_1})$, for any $q(n, m)$

2. for $i = 1$ to n_{it}

   (a) for $l = 2$ to M
      i. $f(n, m, p_l) = DFT^{-1}\{DFT\{f(n, m, p_{l-1})\}H_1(n_f, m_f)\}$
      ii. $f(n_{\mathbf{i}_l}, m_{\mathbf{i}_l}, p_l) = \mathbf{v}_l$
   (b) end
   (c) $f(n, m, 1) = DFT^{-1}\{DFT\{f(n, m, p_M)\}H_{-M+1}(n_f, m_f)\}$
   (d) $f(n_{\mathbf{i}_1}, m_{\mathbf{i}_1}, 1) = \mathbf{v}_1$;

3. end

where $\mathbf{v}_l$ is the vector of the known samples on the plane $z = p_l X_s$, and i_l and $\bar{i}_l$ are the vector of indices of the known and the unknown values on the plane $z = p_l X_s$, respectively. $q(n, m)$ is an arbitrary function whose samples are used in place of the unknown samples and n_{it} is the number of total iteration [2].

3.2. Conjugate Gradient

The second algorithm is based on Eq. 3 which provides the relation between the complex amplitudes of the plane waves, $A_D(n_f, m_f)$, and the given data samples. The relationship given by Eq. 3 can be expressed as a matrix multiplication,

$$\mathbf{u} = \mathbf{R}\mathbf{a} \tag{7}$$

where the vector **a** denotes the complex amplitudes of the plane waves that form the diffraction field on the reference plane. In Eq. 3, these complex amplitudes, $\mathbf{A}_D(n_f, m_f)$, are given as a 2D array, $\mathbf{A}_D = [\mathbf{a}_1|\mathbf{a}_2|\ldots|\mathbf{a}_N]$. The representation of $\mathbf{A}_D$ is converted into a vector, **a**, in Eq. 7 as

$$\mathbf{a} = \begin{bmatrix} \mathbf{a}_1 \\ \hline \mathbf{a}_2 \\ \hline \vdots \\ \hline \mathbf{a}_N \end{bmatrix}. \tag{8}$$

The vector **u** in Eq. 7 denotes the diffraction field on the given data points. The **R** matrix in Eq 7 is the reconstruction matrix and its elements are

$$\mathbf{r}_{l,i,j} = \exp\left(j\sqrt{k^2 - (\frac{2B}{N}i)^2 - (\frac{2B}{N}j)^2}z_l\right)$$
$$\exp\left(j\frac{2B}{N}ix_l\right)\exp\left(j\frac{2B}{N}jy_l\right) \tag{9}$$

where x_l and y_l are the locations of the given samples on the plane $z = z_l$. The **R** matrix is formed as in Eq. 10.

Multiplication of **u** by the pseudo-inverse of the **R** will give **a**. The pseudo-inversion of the matrix **R** is taken by CG algorithm. The method is summarized as

$$\mathbf{R} = \begin{bmatrix} \mathbf{r}_{1,1,1} & \cdots & \mathbf{r}_{1,N,1} & \mathbf{r}_{1,1,2} & \cdots & \mathbf{r}_{1,N,2} & \cdots & \mathbf{r}_{1,1,N} & \cdots & \mathbf{r}_{1,N,N} \\ \mathbf{r}_{2,1,1} & \cdots & \mathbf{r}_{2,N,1} & \mathbf{r}_{2,1,2} & \cdots & \mathbf{r}_{2,N,2} & \cdots & \mathbf{r}_{2,1,N} & \cdots & \mathbf{r}_{2,N,N} \\ & \vdots & & & \vdots & & \ddots & & \vdots & \\ \mathbf{r}_{s,1,1} & \cdots & \mathbf{r}_{s,N,1} & \mathbf{r}_{s,1,2} & \cdots & \mathbf{r}_{s,N,2} & \cdots & \mathbf{r}_{s,1,N} & \cdots & \mathbf{r}_{s,N,N} \end{bmatrix}. \tag{10}$$

1. compute the $\mathbf{R}$ by using Eq. 9 and Eq. 10

2. if $s < N^2$ compute $\mathbf{Q} = \mathbf{R}\mathbf{R}^H$ and $\mathbf{b} = \mathbf{u}$, otherwise compute $\mathbf{Q} = \mathbf{R}^H\mathbf{R}$ and $\mathbf{b} = \mathbf{R}^H\mathbf{u}$

3. initialize $\hat{\mathbf{x}}^{[0]}$ arbitrarily, $\mathbf{d}_0 = \mathbf{b} - \mathbf{Q}\hat{\mathbf{x}}^{[0]}$ and $\mathbf{g}_0 = -\mathbf{d}_0$

4. for $n = 1$ to $n_{it} \leq N^2$

    (a) $\alpha_n = -\dfrac{\mathbf{g}_n^T \mathbf{d}_n}{\mathbf{d}_n^T \mathbf{Q} \mathbf{d}_n}$

    (b) $\hat{\mathbf{x}}^{[n+1]} = \hat{\mathbf{x}}^{[n]} + \alpha_n \mathbf{d}_n$

    (c) $\mathbf{g}_{n+1} = \mathbf{Q}\hat{\mathbf{x}}^{[n+1]} - \mathbf{b}$

    (d) $\gamma_n = -\dfrac{\mathbf{g}_{n+1}^T \mathbf{d}_n}{\mathbf{d}_n^T \mathbf{Q} \mathbf{d}_n}$

    (e) $\mathbf{d}_{n+1} = -\mathbf{g}_{n+1} + \gamma_n \mathbf{d}_n$

5. if $s < N^2$ compute $\hat{\mathbf{a}} = \mathbf{R}^H\hat{\mathbf{x}}$, otherwise $\hat{\mathbf{a}} = \hat{\mathbf{x}}$

6. reconstruct the diffraction field on the reference plane from the estimated complex amplitudes of the plane waves by utilizing inverse FT relation.

4. RESULTS

The outlined algorithms are evaluated by a synthetically generated simple optical field on the reference plane. Then, the diffraction field over the 3D space, due to the diffraction field on the reference plane, is computed according to Eq. 6. The field on the reference plane consists of N by N samples, where $N = 64$. There is an 8 by 8 unit-magnitude rectangular opening located in the middle of the reference plane and the rest of the samples are taken as zero. The 3D space consists of $M = 64$ planes which are uniformly located along the $\mathbf{z}$-axis and there is a 64 by 64 uniform grid on each plane. An illustration of the implemented scenario is given in Figure 1. In the scenario, the distance parameter p between the reference and first plane equals to four and there are M planes in the defined 3D space. Typical results of the algorithms can be seen in Figure 2.

Evaluation of the results is based on two parameters. One of them is the normalized error between the original and the reconstructed diffraction patterns, $u(n,m,0)$ and $u'(n,m,0)$:

$$\left(\sum_{n,m=0}^{N-1} |u'(n,m,0) - u(n,m,0)|^2 \right) \bigg/ \left(\sum_{n,m=0}^{N-1} |u(n,m,0)|^2 \right). \tag{11}$$
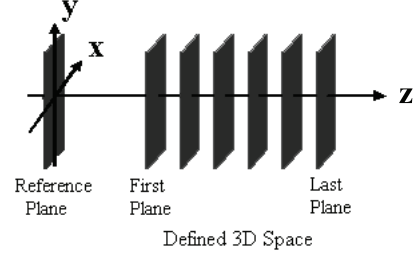
Fig. 1. Implemented scenario.

The other one is the number of complex multiplications required by the algorithms. From the computed field over the 3D space, we randomly take s data points to reconstruct the field on the reference plane. For each value of s, ten different random selections of data points are generated, assessment parameters are computed for each selection and then averaged for each value of s.

Increasing the number of given samples, s, in both algorithms provides faster convergence to the given field on the reference plane, as expected. The curves in Figure 3 show how fast the normalized errors decrease when the number of complex multiplications is fixed to 1.7×10^9.

When $s \leq N^2$, the solution sets of the algorithms will not be comprised by only the original field. Hence, the solution may converge to pattern which may not be the same as the original one.

The computational complexities of both algorithms are determined by the number of complex multiplications, because we assume that complex multiplication needs more computation time than complex addition, data fetching and writing operations. Both algorithms use the 2D-DFT operation which can be implemented by $N^2 \log_2 N$ complex multiplications if common 2D-FFT algorithms are used. For the POCS algorithm, total number of complex multiplications is

$$n_{it}(2MN^2 \log_2 N + N^2 M). \tag{12}$$

The parameter n_{it} is related to the s, but there is no closed form for it. It can be found from the experiments. For the CG algorithm, the total number of complex multiplications is

$$2n_{it}N^4 + sN^2 + N^2 \log_2 N \tag{13}$$

where the parameter n_{it} is again heuristically estimated. It is found by the numerical experiments for each scenario. The curves in Figure 4 illustrate the necessary complex multiplications in POCS and CG algorithms.
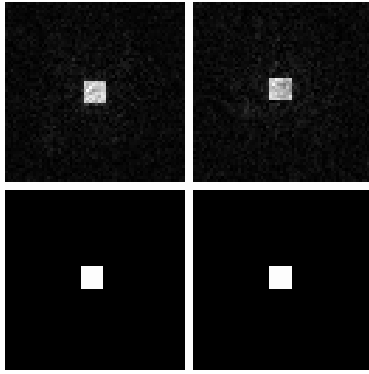
Fig. 2. Layout of the figure $\left|\frac{a}{c}\right|\frac{b}{d}\right|$ (a) Magnitude of the reconstructed diffraction field on the reference plane obtained by the POCS algorithm when the number of given samples is $0.8N^2$. (b) The same scenario as in (a) when CG is used (c) Reconstructed field by POCS on the same plane when the number of given samples is $2.0N^2$. (d) The same scenario as in (c) when CG is utilized.

5. CONCLUSION

Two effective methods to calculate the scalar optical diffraction field simultaneously due to the arbitrarily distributed sample points over the 3D space are presented. First method utilizes POCS algorithm and the second one is based on CG algorithm. Both of them are iterative methods. POCS needs less memory space than CG. In CG, we have to use large matrices to represent the diffraction field relationship. Implementation of POCS needs less number of complex multiplications than CG in the case, when the given 3D diffraction field samples are taken from an uniform grid with large enough sampling period over the **z**-axis.

Fig. 3. Convergence of the POCS and the CG algorithms for different number of known samples at approximately 1.7×10^9 complex multiplications. These curves are obtained by averaging the results of 10 simulations. Solid line stands for the POCS, dashed line is used for the CG.
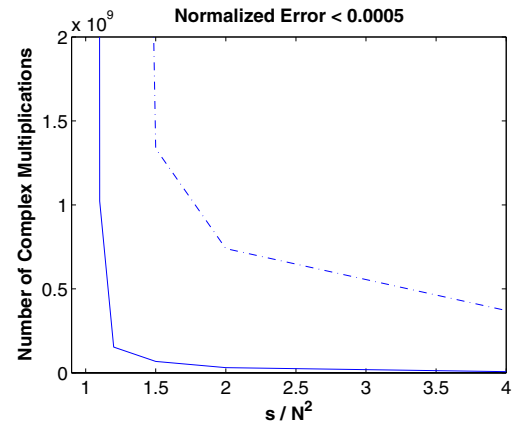
Fig. 4. Number of complex multiplications for POCS and CG methods when the normalized error is limited to 0.0005. The given results are based on the average of 10 simulations. Solid line represents the POCS, dashed line indicates the CG.

6. REFERENCES

[1] J. W. Goodman, *Introduction to Fourier Optics*, McGraw-Hill, New York, 1996.

[2] G.B. Esmer, V. Uzunov, L. Onural, H.M. Ozaktas, and A. Gotchev, "Diffraction field computation from arbitrarily distributed data points in space," *Signal Processing: Image Communication (2006)*.

[3] V. Uzunov, A. Gotchev, G. B. Esmer, L. Onural, and H. M. Ozaktas, "Non-uniform sampling and reconstruction of diffraction field," in *In Workshop on Spectral Methods and Multirate Signal Processing, SMMSP 2006, volume TICSP Series 34*, 191-198, September 2006.

[4] G. C. Sherman, "Application of the convolution theorem to Rayleigh's integral formulas," *J. Opt. Soc. Am.*, vol. 57, pp. 546–547, 1967.

[5] Levent Onural, "Impulse functions over curves and surfaces and their applications to diffraction," *J. Math. Anal. Appl.*, vol. 322, pp. 18–27, 2006.

[6] G. Bora Esmer and Levent Onural, "Computation of holographic patterns between tilted planes," in *Holography 2005*, Varna, Bulgaria, 21-25, May 2005, vol. Proc. SPIE 6252.